Optical properties of porous silicon. Part III: Comparison of experimental and theoretical results

Andrea Edit Pap [a,*], Krisztián Kordás [a], Jouko Vähäkangas [a], Antti Uusimäki [a],
Seppo Leppävuori [a], Laurent Pilon [b], Sándor Szatmári [c]

[a] *Microelectronics and Materials Physics Laboratories, Department of Electrical and Information Engineering,
University of Oulu, P.O. Box 4500, FIN-90014 Oulu, Finland*
[b] *Mechanical and Aerospace Engineering Department, University of California, Engineering IV Room 46-147C,
Los Angeles, CA 90095-1597, USA*
[c] *Department of Experimental Physics, University of Szeged, 6720-H Szeged, Dóm tér 9, Hungary*

Abstract

In our previous study, the refractive indices of freestanding porous silicon (PS) layers were derived using the envelope method, where the computation is based on the values of local minima and maxima in the oscillations of transmission spectra. In the present work, an improved procedure for calculating the optical parameters from the measurements data is described. It is verified by reflection measurements on freestanding samples that optical scattering at the air–PS interface is the main reason for the loss of the transmitted light intensity and thus for the inaccurate results we obtained earlier by the envelope method. This however can be avoided by taking into consideration the relationship between the optical path in the plane-parallel film and the position of extrema in the transmission spectra. The as-determined effective refractive indices show very good matching with the theoretical calculations by the Bruggeman's effective medium approximation.
© 2005 Elsevier B.V. All rights reserved.

1. Introduction

The optical properties of a porous silicon (PS) layer produced by electrochemical etching are determined by the thickness, porosity and by the shape and size of pores [1,3–5]. These structural parameters strongly depend on the manufacturing conditions such as current density, etching time, electrolyte composition, and also on the dopant type and concentration of the original

Si wafer [3–7]. Generally, the PS materials are described as a homogenous mixture of air, silicon and in some case, silicon dioxide. From the optical point of view, in the visible and infrared wavelength range, PS can be specified as an effective medium, whose optical properties depend on the relative volumes of silicon, pore filling medium and in some cases silicon oxide, i.e. mainly on the porosity and on the degree of oxidation of the PS layer [5].

The optical properties of PS layers can be determined using both experimental and model based approaches [8]. In the case of experimental methods, one can record the transmission or reflection spectra and the parameters

---

* Corresponding author. Tel.: +358 8 5532741; fax: +358 8 5532728.
E-mail address: papa@ee.oulu.fi (A.E. Pap).

are calculated using for example the envelope method [9,10] or the Fresnel's equation. Unfortunately, these procedures are limited when the materials investigated show strong optical absorption and/or scattering. In the case of semi-empirical approaches the refractive indices are measured using spectroscopic ellipsometry and then the model parameters such as layer thickness and calculated effective dielectric function are adjusted to fit the experimental spectra by the use of a suitable model [5,8,11]. Another semi-empirical way is provided if a PS Fabry–Perot interferometer is fabricated and measured, and using the transfer matrix method the optical parameters are varied to find the best fit of the model to the measured spectra [5,8,12]. Fully theoretical solutions are provided by different effective medium approximation (EMA) methods such as Maxwell–Garnett's, Looyenga's or Bruggeman's [5,8,14]. Note that these approximations are valid only for certain circumstances, thus might lead to different results, when calculating the index of refraction for a given porous system.

In this work, various calculation methods based on optical transmission and reflection measurements are used to extract the refractive index data for freestanding PS layers. The calculated refractive indices are compared with the theoretical ones obtained by Bruggeman's effective medium approximation. Moreover, the limitations of the envelope method and the accuracy of the measurements are investigated and described.

2. Experimental

2.1. Sample preparation and characterization

PS layers with various porosities were fabricated by electrochemical etching of boron-doped Si wafers (0.015 Ω cm) in the mixture of hydrofluoric acid and eth-

anol. The experimental parameters applied in the anodization process are collected in Tables 1 and 2. The samples for transmission measurements were relatively thin (3.6–14.4 μm) freestanding layers of PS. The films were detached from the wafer by an electrochemical polishing step (J_{pol} = 500 mA/cm^2, τ = 10 s) after the anodization process. For the reflection measurements thick ($\sim$200 μm) freestanding layers were prepared each having an anti-reflection layer (porosity gradient) on its back side. This was obtained by increasing gradually the anodization current density at the end of the anodization process in 6.5 mA/cm^2 steps at every 2 s until J_{pol} = 500 mA/cm^2 is reached. After preparation, every single sample was flushed separately in absolute ethanol and stored in pentane until the optical measurements.

In order to determine the porosity of PS samples and the anodization rate of electrochemical process, control samples were fabricated and investigated. After stripping the samples in 1 M NaOH aqueous solution, the depth of grooves in Si was measured by a Dektak^3 ST surface profiler. The thickness of a stripped layer equals to that of a dissolved PS layer. Direct thickness measurements of freestanding PS layers were carried out by optical microscopy with a relative standard deviation (RSD) of 1.5% $\leqslant$ RSD $\leqslant$ 3.8%. The porosity of samples was calculated as the fraction of void within the porous layer, i.e. $p = (m_1 - m_2)/(m_1 - m_3)$ where m_1, m_2 and m_3 denote the mass of the original, anodized and stripped wafer, respectively. Due to the limited accuracy of mass measurements and the limited repeatability of sample preparation, the relative standard deviation in the porosity, is within the range of 0.5% $\leqslant$ RSD $\leqslant$ 2.2%.

In our previous work [1], an electrolyte concentration of 11.7 M HF and 10.3 M C$_2$H$_5$OH was applied, and the current densities were set to 20, 35, 50 and 65 mA/cm^2. The calculated porosities for those samples were lower compared to the current PS layers, whereas the etching

Table 1
Preparation conditions and corresponding physical properties of freestanding PS layers for transmission measurements

Electrolyte composition	Current density (J)	Etching time (τ)	Porosity ($\bar{p} \pm \Delta\bar{p}$)	Thickness ($\bar{t} \pm \Delta\bar{t}$)
14.55 M HF and 8.5 M C$_2$H$_5$OH	20 mA/cm^2	135 s	40.56% ± 0.51%	3.6 μm ± 0.1 μm
11.7 M HF and 10.3 M C$_2$H$_5$OH	20 mA/cm^2	800 s	46.57% ± 1.04%	12.9 μm ± 0.3 μm
11.7 M HF and 10.3 M C$_2$H$_5$OH	35 mA/cm^2	400 s	51.92% ± 0.73%	14.3 μm ± 0.3 μm
11.7 M HF and 10.3 M C$_2$H$_5$OH	50 mA/cm^2	250 s	57.43% ± 0.74%	11.3 μm ± 0.2 μm
11.7 M HF and 10.3 M C$_2$H$_5$OH	65 mA/cm^2	260 s	60.50% ± 0.28%	14.4 μm ± 0.2 μm

Table 2
Preparation conditions and corresponding physical properties of freestanding PS layers for reflection measurements

Electrolyte composition	Current density (J)	Etching time (τ)	Porosity ($\bar{p} \pm \Delta\bar{p}$)	Thickness (t)
14.55 M HF and 8.5 M C$_2$H$_5$OH	20 mA/cm^2	7380 s	40.56% ± 0.51%	$\sim$200 μm
11.7 M HF and 10.3 M C$_2$H$_5$OH	20 mA/cm^2	8420 s	46.57% ± 1.04%	$\sim$200 μm
11.7 M HF and 10.3 M C$_2$H$_5$OH	35 mA/cm^2	6220 s	51.92% ± 0.73%	$\sim$200 μm
11.7 M HF and 10.3 M C$_2$H$_5$OH	50 mA/cm^2	3770 s	57.43% ± 0.74%	$\sim$200 μm
11.7 M HF and 10.3 M C$_2$H$_5$OH	65 mA/cm^2	3450 s	60.50% ± 0.28%	$\sim$200 μm

rates are found similar. For the recent samples, the mass of the Si skeleton ($m_2 - m_3$) fits well to the mass calculated from the porosity and geometry of films $m_2 - m_3 = \rho_{Si} t r^2 \pi (1 - p)$, where r is the radius of the porous silicon samples and ρ_{Si} is the density of crystalline silicon. This matching validates the recent porosity measurements, and suggests that a systematic error was made when measuring mass in our previous work. On the other hand, the previously published refractive index values and absorption coefficients were not affected by the error of these parameters. This is due to the method for calculating the optical coefficients from the recorded transmission spectra (envelope method).

2.2. Optical measurements

Optical transmission and reflection measurements were carried out in the 700–1700 nm spectral range in ambient air using an ANDO AQ-6315 optical spectrum analyzer. The accuracy of optical measurements was enhanced by repeating and averaging twenty measurements for each wavelength for data acquisition and also small step sizes (0.2 nm) for scanning the wavelength range with the monochromator. The experimental arrangements used for optical transmission and reflection measurements are drafted in Fig. 1.

The optical transmittance T was calculated from the measured transmitted light intensity through the free optical path I_0 and samples I_S, $T = I_S/I_0$. In the reflection measurements, the reference intensity $I_{M(0)}$ was set up using a gold mirror in the position of the sample. The reflected intensity from the mirror I_M was measured and then corrected for the wavelength dependent reflectivity of the mirror f_C (Edmund Optics Ltd., Optics and Optical Instruments Catalog, 2004, p. 98) as $I_{M(0)} = I_M/f_C$. Thus the reflectivity of the samples R is obtained as $R = I_S/I_{M(0)}$, where I_S is the reflected intensity from the PS films. (Note that, I_0, I_S and I_M are on a linear scale.)

3. Results and discussion

The envelope method [9] gives a simple solution to calculate the optical parameters of a thin transparent dielectric film from a measured transmission T spectrum in a non-absorbing surrounding medium. Using the oscillations of T, the refractive index n_{PS}^{env} of a thin film is:

$$n_{PS}^{env} = (N + (N^2 - n_0^2 n_1^2)^{0.5})^{0.5}, \qquad (1)$$

where

$$N = \frac{n_0^2 + n_1^2}{2} + 2n_0 n_1 \frac{T_{max} - T_{min}}{T_{max} T_{min}}. \qquad (2)$$

The T_{max} and T_{min} are the envelope functions of the local minima and maxima in the transmission spectrum; n_0 and n_1 are the refractive indices of media in front and behind the film. (In our measurements $n_0 = n_1 = 1$.)

In our previous study [1], four types of freestanding PS membranes of different porosities were manufactured
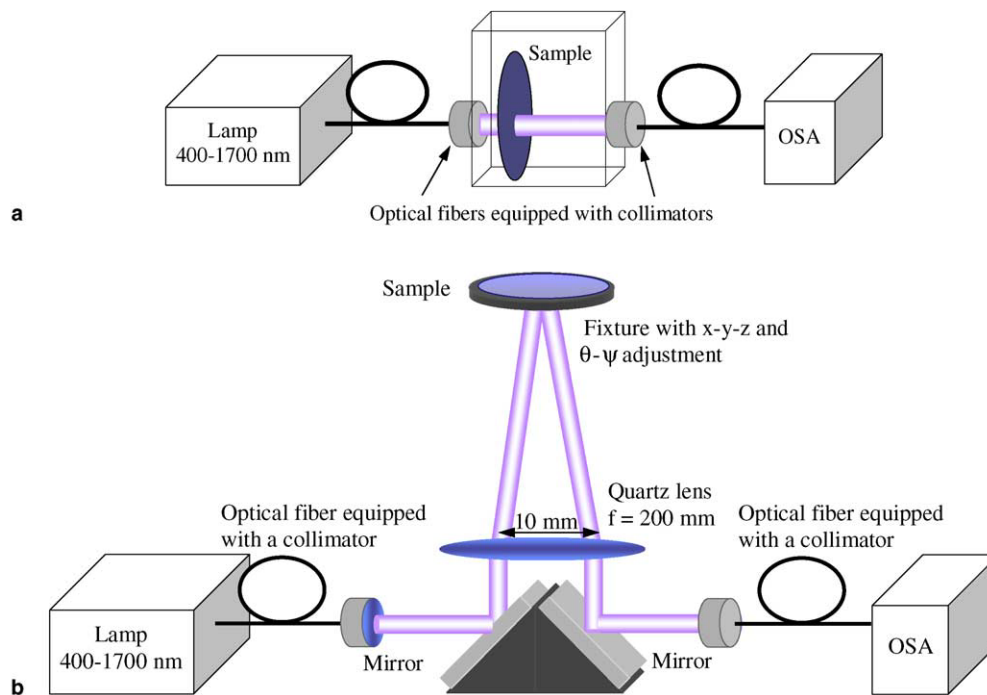

Fig. 1. Schematics of experimental setups used for optical (a) transmission and (b) reflection measurements. The transmitted beam is perpendicular to the sample, while in the reflection measurements the angle of incidence is ∼88.5°.

and their optical transmission was measured. It was observed that with increased membrane porosity, the transmitted light intensity increases and the refractive index decreases. The membranes had poor transparency at shorter wavelengths ($\lambda < 800$ nm) because of the fundamental optical absorption in Si. The calculated
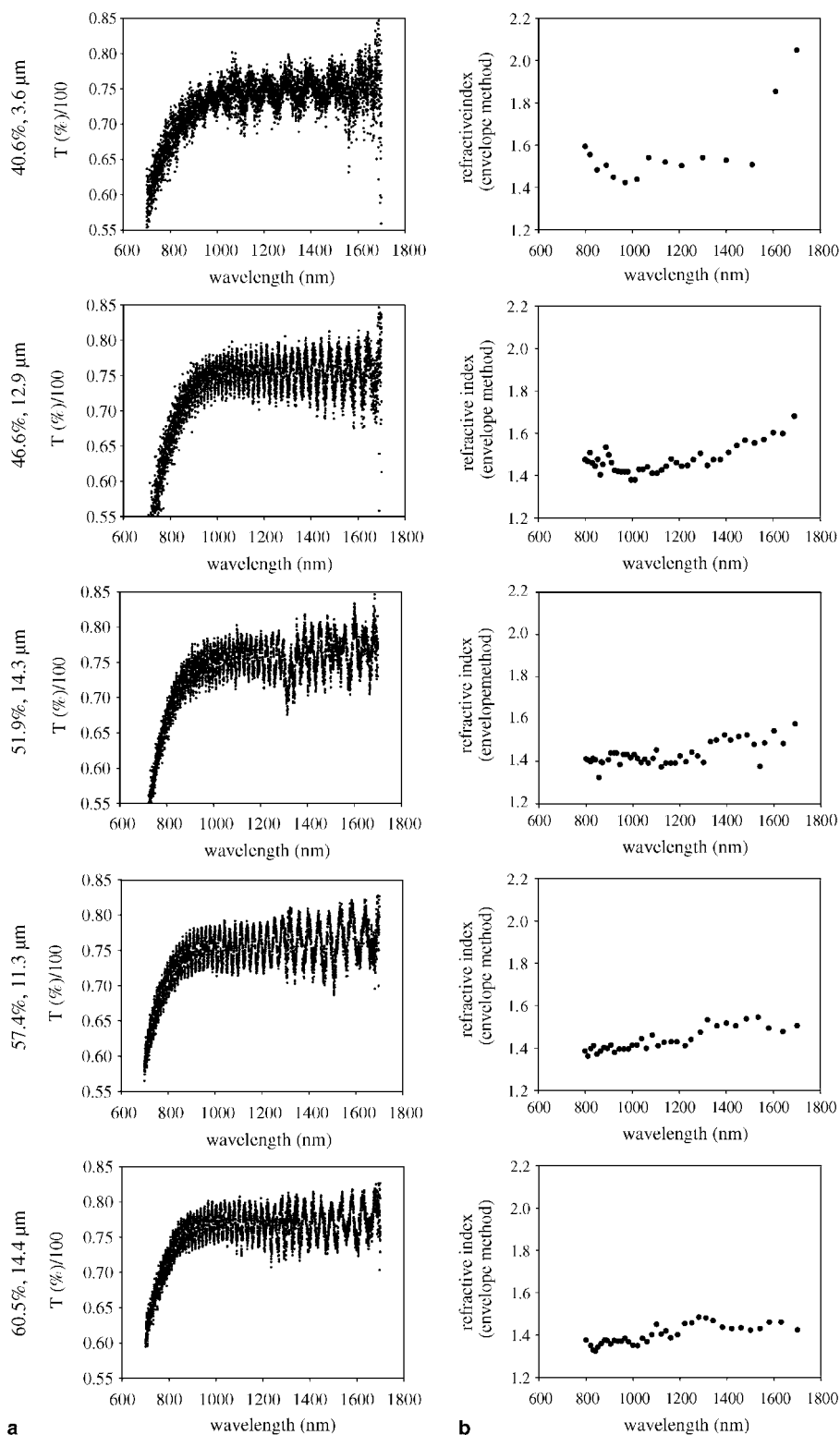

Fig. 2. (a) Transmission spectra of freestanding PS films with different porosity and thickness and (b) the corresponding refractive indices calculated using the envelope method.

refractive indices ($\lambda > 800$ nm) of PS films were in qualitative agreement with those expected by the effective medium theory (i.e. a higher porosity results in lower index of refraction and vice versa). On the other hand the values extracted from the measurements by the envelope method were lower (factor of ~ 0.6) than those calculated with Bruggeman's theory. In addition, unexpected anomalous dispersion of the index of refraction was also observed. Clear explanation of these results could not be revealed.

In our current work, both sample preparation and transmission measurements with much higher accuracy have been repeated. Thinner plane-parallel freestanding films have been created (~ 12 μm instead of ~ 30 μm) to decrease the frequency of oscillations in the recorded transmission spectra. In order to increase the resolution of optical measurement, the step of wavelength scanning was shortened (from 1.3 nm to 0.2 nm) and higher number of averaging was used for data acquisition (20 instead of 9). In Fig. 2, the recorded transmission spectra and the corresponding calculated (envelop method) refractive indices are collected for five different PS films. As it can be seen, the current results are in good agreement with the previous study [1]: the computed refractive indices are still lower than it could be expected from the effective media, and show anomalous dispersion. Note that the reliability of the measurement is significantly improved for shorter wavelengths than 1000 nm as compared to the previous study.

The results of the repeated experiments and calculations suggest that the source of anomalies is in the envelope method itself. The values of n_{PS}^{env} given by the envelope method depend on T_{max} and T_{min}. If one obtains a lower n_{PS}^{env} than expected, it means the envelope functions are not opened up: T_{max} is lower and T_{min} is higher compared to the real case. Physically, this can be attributed to optical losses (absorption and scattering) when measuring the transmittance of the samples. Since the envelope method includes the parameter of absorption (for weekly absorbing media) the only plausible explanation for the supposed losses is an optical scattering in the porous media. Additionally, the experienced anomaly in the refractive indices suggests that the extent of the light scattering is lower in the IR then in the visible.

To verify our presumption, besides the transmission spectra, optical reflection spectra were recorded. To minimize the back-side reflection, freestanding PS layers of ~ 200 μm thickness with anti-reflection layer on the back-side were fabricated (Fig. 3(a)). The porosity of the samples was the same as those used in the transmission measurements (within the repeatability of sample preparation). The reflectivity of a polished Si wafer was also measured and used for further calculations:

– First, the refractive index dispersion curve for $n_{Si}^{Fresnel}$ is determined using Fresnel's equation for an
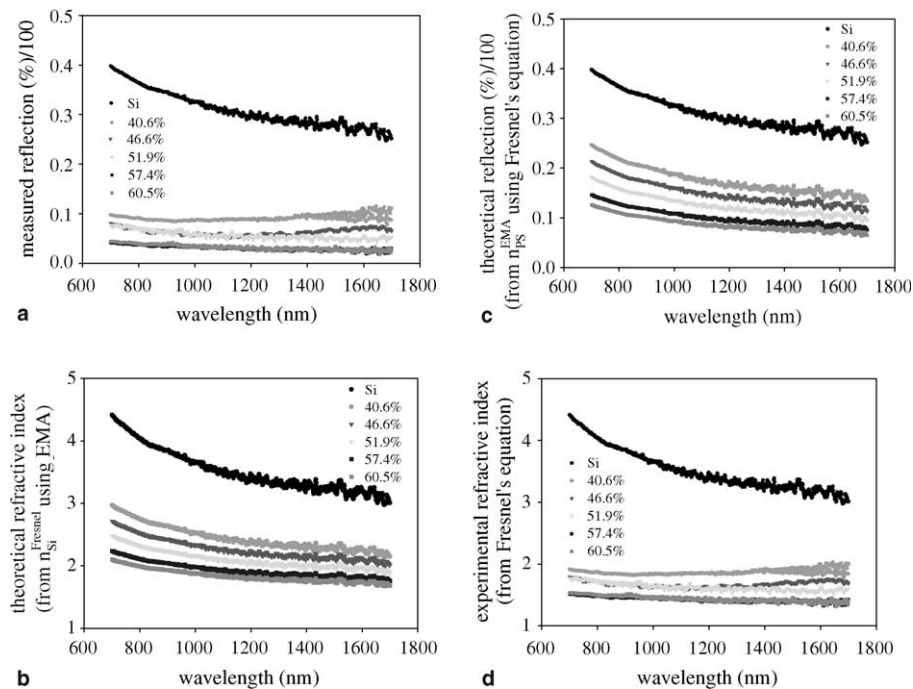

Fig. 3. (a) Measured reflectivity of Si and PS samples. (b) Calculated index of refraction for Si from the reflection measurements, and derived effective refractive indices for the porous samples. (c) Calculated theoretical reflection using the theoretical effective refractive indices. (d) Refractive indices calculated from measured optical reflection.

air-Si interface $R_{Si} = (n_{Si}^{Fresnel} - 1)^2/(n_{Si}^{Fresnel} + 1)^2$, i.e. $n_{Si}^{Fresnel} = (\sqrt{R_{Si}} + 1)/(\sqrt{R_{Si}} - 1)$.

– In the second step, from $n_{Si}^{Fresnel}$ the index of refraction for the effective media n_{PS}^{EMA} is calculated from Bruggeman's effective medium approximation. Bruggeman's theory describes the dielectric constant of a two-component materials system:

$$f \frac{\varepsilon_1 - \varepsilon_{eff}}{\varepsilon_1 + 2\varepsilon_{eff}} + (1 - f)\frac{\varepsilon_2 - \varepsilon_{eff}}{\varepsilon_2 + 2\varepsilon_{eff}} = 0, \tag{3}$$

where f is the volume fraction of one of the components, ε_1 and ε_2 are the dielectric functions of the components and ε_{eff} is the effective dielectric function of the mixed material. From the Maxwell's equations the dielectric permittivity is $\varepsilon = n^2 - k^2$ where k is the extinction coefficient. For a transparent or a weakly absorbing medium $k \ll n$, thus we get $n = \sqrt{\varepsilon}$, [13]. Accordingly, the effective refractive index is described with

$$p \frac{n_{pore}^2 - n_{PS}^2}{n_{pore}^2 + 2n_{PS}^2} + (1 - p)\frac{n_{Si}^2 - n_{PS}^2}{n_{Si}^2 + 2n_{PS}^2} = 0 \tag{4}$$

since the volume fraction of voids equals to the porosity of our samples $f = p$. Thus, for the mixture of air and Si [14] (Fig. 3(b)) we get

$$n_{PS}^{EMA} = 0.5\left[3p(1 - n_{Si}^2) + (2n_{Si}^2 - 1)\right.$$
$$\left. + \left((3p(1 - n_{Si}^2) + (2n_{Si}^2 - 1))^2 + 8n_{Si}^2\right)^{0.5}\right]^{0.5}. \tag{5}$$

– From the as-obtained n_{PS}^{EMA} values the theoretical reflectivity of the corresponding effective media can be calculated using the Fresnel's equation again (Fig. 3(c)).
– Another series of refractive indices can be determined from the measured reflectivities of the porous samples by $n_{PS}^{Fresnel} = (\sqrt{R_{PS}} + 1)/(1 - \sqrt{R_{PS}})$ (Fig. 3(d)).

The difference between the experimental (Fig. 3(a)) and theoretical (Fig. 3(c)) reflectivities is considerable. At shorter wavelengths, the measured reflectivity is significantly lower than the theoretical one, though the dif-

ference tends to decrease for longer wavelengths. It also supports our presumption about the scattering phenomena. Namely, considering a typical feature size of $d \sim 30$ nm for the pore diameters and Si wall thickness in the skeleton, the size parameter $a = \pi d/\lambda$ is between ~ 0.13 and ~ 0.06 for the applied wavelength range. Such size parameter satisfies the criterion for Rayleigh scattering, where the scattered intensity is proportional to a^4. It means that the scattered intensity is about 30 times smaller than that for 700 nm, which seems to be in agreement with the phenomena observed in the reflection spectra of PS films.

In order to visualize the scattering on the porous surface, a PS sample and a pristine Si bulk were illuminated using a visible HeNe laser beam (633 nm, TEM$_{00}$). In the case of the PS surface, the spot of the incident laser beam can clearly be seen from any direction indicating that light is scattered in the whole solid angle (Fig. 4(a)) according to the isotropic nature of Rayleigh scattering. On the contrary, the surface of a pristine Si wafer behaves as a secularly reflecting mirror: the spot of the incident laser beam is practically invisible from any direction different from the optical axes (Fig. 4(b)).

The reflection measurement has demonstrated the presence of light scattering on the PS surface, but did not solve the computation problem. The methods (i.e. envelope method as well as calculation from Fresnel's reflection) used to recover the refractive indices from the recorded transmission and reflection spectra failed to provide accurate data. Both methods lack to handle the intensity loss caused by scattering.

One can overcome such limitations by introducing a method, which is not affected by the losses. Considering the fact that the positions of extrema in the transmission spectra are fairly independent from both scattering and absorption, we can utilize the well-known relationship between the layer thickness t, the refractive index and the positions of extrema $n_{PS}^{int} = M\lambda_1\lambda_2/2t(\lambda_2 - \lambda_1)$ [5,8,9]. Here, M is the number of oscillations (fringes) between two extrema at λ_1 and λ_2. This equation is also used in the envelope method, when the extraction of layer thickness is aimed from the previously calculated refractive indices. However, we suggest an opposite approach: after determining the layer thickness of samples
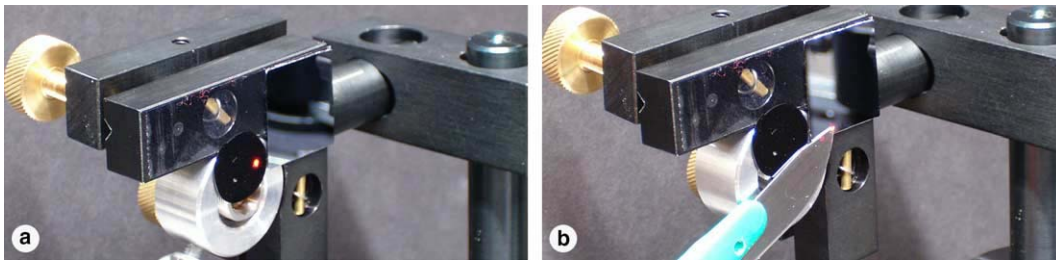

Fig. 4. Demonstration of light scattering from the surfaces of a porous silicon film (a) and from pristine wafer (b). In the latter case, the beam is shown with the apex of scalpel.

by microscopy we calculate the refractive indices of the freestanding PS layers from the positions of adjacent maxima or minima in the recorded optical transmission spectra (Fig. 5). The values obtained from the positions
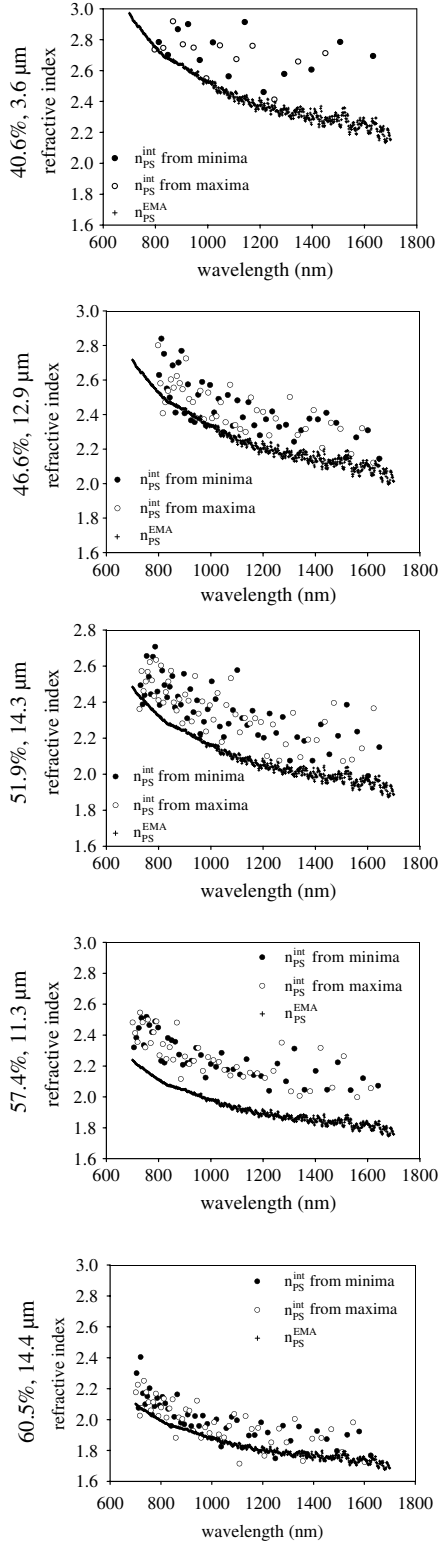

Fig. 5. Refractive indices of PS layers as-calculated from the positions of extrema in the transmission spectra and from Bruggeman's EMA.

of minima are in excellent agreement with those obtained from the wavelengths of maxima. The as-extracted results show good matching with those obtained by theoretical considerations, which means that the effective index of refraction for the mixture of nano-porous Si and air follows the Bruggeman's effective medium theory. It is worth noting that the experimentally retrieved index of refraction is always larger than that predicted by the Bruggeman's method. The mean of relative difference between the experimental and theoretical values is 9.1% with a standard deviation of 4.4%. The minimum and maximum differences are 1.5% and 17.6%, respectively.

Now, by using the accurate refractive indices, one can approximate the corresponding values of T_{max} and T_{min} envelopes for the idealized transmission spectra using Eqs. (1) and (2). By substituting the measured PS layer thickness, the accurate index of refraction and the approximated T_{max} and T_{min} values into

$$\alpha = -\frac{1}{t} \ln \frac{(n+n_0)(n_1+n)(1-(T_{max}/T_{min})^{0.5})}{(n-n_0)(n_1-n)(1+(T_{max}/T_{min})^{0.5})} \quad (6)$$

one gets the approximated absorption coefficients for the PS film [9]. These values are typically similar or slightly smaller compared to those we can calculate directly by Eqs. (1) and (2) from the experimental observations (see Fig. 2).

In Ref. [2] various Bragg reflectors based on periodically alternated porous silicon layers were fabricated and analyzed. The calculation of the Bragg conditions $\lambda_{Bragg} = \frac{2}{m}(n_L t_L + n_H t_H)$ was based on the refractive indices extracted by the envelope method [1]. Using typical layer thickness values of $t_H \sim 440$ nm and $t_L \sim 450$ nm for the layers having higher n_H and lower n_L index of refraction, the Bragg orders m for the stop bands in the measured 400–1700 nm spectrum ranges were calculated. In the spectra, we found a stop band starting close to 1700 nm and another one around 900 nm, both which shift towards the shorter wavelengths when increasing the numbers of alternating periods in the PS stack. The shift of the bands was explained by the decrease of layer thickness when stacks having higher numbers of periods were manufactured; and by the supposed anomalous dispersion of refractive indices. For the stop band appearing at the longer wavelengths m is calculated as a second order reflection. Considering that the refractive indices of PS obtained earlier by the envelope method and the current results for the longer wavelengths are very similar, the current results support that the stop band is the 2nd harmonic of the first Bragg condition. The band appearing around 900 nm—as we concluded earlier—belonged to the 3rd Bragg order. Now, if we take into account that the accurate values for n_{PS} are considerably higher than those calculated earlier for wavelengths close to the visible, we get that the band most likely corresponds to the merged bands of the 4th

and 5th Bragg condition; and the 3rd harmonics is most likely merged with the 2nd one. Finally, the shift and the broadening of reflection bands are due to the thickness variation in the layers and because of the normal dispersion of refractive indices.

4. Conclusions

This paper gives a comparative study on the optical properties of porous silicon layers obtained by various experimental and model-based approaches. In the view of the recent findings the following conclusions are drawn:

– When studying the optical properties of porous media of ~30 nm pore size, one has to consider photon scattering from the pores in the near infrared spectrum.
– If scattering takes place, the optical parameters cannot be derived precisely from the transmission spectra using the envelope method because the values of local extrema in the transmission spectra $T_{max}(\lambda)$ and $T_{min}(\lambda)$ used for calculating the index of refraction, absorption, and film thickness are affected by the scattering losses. Since the relative positions of extrema are fairly independent on the scattering losses, the index of refraction can be precisely calculated from $n_{PS}^{int} = M\lambda_1\lambda_2/2t(\lambda_2 - \lambda_1)$ the criteria of interference for a film of t thickness. The as-calculated refractive indices show normal optical dispersion on the contrary to the anomalous dispersion obtained using the envelope method.
– The as-calculated refractive indices agree well with the Bruggeman's effective medium approximation.

References

[1] K. Kordás, A.E. Pap, S. Beke, S. Leppävuori, Opt. Mater. 25 (2004) 251.
[2] K. Kordás, S. Beke, A.E. Pap, A. Uusimäki, S. Leppävuori, Opt. Mater. 25 (2004) 257.
[3] K. Kordás, J. Remes, S. Beke, T. Hu, S. Leppävuori, Appl. Surf. Sci. 178 (2001) 290.
[4] O. Bisi, S. Ossicini, L. Pavesi, Surf. Sci. Rep. 38 (2000) 1.
[5] L.T. Canham, Properties of Porous Silicon, IEE, INSPEC, London, 1997, pp. 3–43 and 223–246.
[6] S. Zangooie, Fabrication, Characterization and Applications of Porous Silicon Thin Films and Multilayered Systems (Linköping Universitet, SE-581 83, Sweden, 1999) pp. 11–20.
[7] C. Rotaru, N. Tomozeiu, G. Cracium, J. Mol. Struct. 480–481 (1999) 293.
[8] W. Theiss, Surf. Sci. Rep. 29 (1997) 97.
[9] J.C. Manifacier, J. Gasiot, J.P. Fillard, J. Phys. E 9 (1976) 1002.
[10] Y. Laghla, E. Sched, Thin Solid Films 306 (1997) 67.
[11] G.E. Jellison Jr., F.A. Modine, J. Appl. Phys. 76 (1994) 3758.
[12] J. He, M. Cada, Appl. Phys. Lett. 61 (1992) 2150.
[13] J.I. Pankove, Optical Processes in Semiconductors, Prentice-Hall, Inc. Englewood Cliffs, New Jersey, 1971, pp. 87–91.
[14] H.F. Arrand, Optical Waveguides and Components Based on Porous Silicon, University of Nottingham, UK, 1997, pp. 63–66.